JOURNAL OF CATALYSIS 130, 147–160 (1991)

The Effects of Transition Metal Oxides on the Methane Oxidative Coupling Activity of Doped MgO Catalysts

I. Zinc and Manganese

F. P. LARKINS[1] AND M. R. NORDIN[2]

Department of Chemistry, University of Tasmania, GPO Box 252C, Hobart, Tasmania 7001, Australia

Received May 30, 1990; revised October 12, 1990

Magnesium oxide samples doped with different loadings of zinc and manganese oxides with and without lithium carbonate being present in the preparation were evaluated for their catalytic activity towards the oxidative coupling of methane to higher hydrocarbons. When Li_2CO_3 is excluded, the exhaustive reactions of methane to form carbon oxides are favoured. With a doped Li_2CO_3/MgO catalyst, a methane conversion of >25% and a selectivity to C_2 hydrocarbons of near 60% was retained but not enhanced in the presence of different loadings of Zn oxide at 805°C. Low loading of Mn oxide on Li_2CO_3/MgO resulted in a methane conversion of >35% and a selectivity to C_2 hydrocarbons of near 50%. At high Mn oxide loadings the methane conversion decreases and the C_2 selectivity is less than 30% due to more exhaustive oxidation. The activity of the doped catalyst is related to the physico-chemical properties, especially surface morphology, and metal oxide reducibility on the basis of SEM, XRD, TRP, and electron microprobe analysis.

1. INTRODUCTION

It has been demonstrated by Driscoll and Lunsford (*1*) that when methane was passed over MgO or Li_2CO_3-doped MgO at 500°C in the presence of oxygen C_2 hydrocarbons were formed. Furthermore, Ito and Lunsford (*2*) reported that a methane conversion of 37.5% with a C_2 selectivity of 46.5% was achieved at 770°C. The catalytic efficiency of the Li_2CO_3/MgO system has been confirmed by others (*3–5*).

The doping of MgO with alkali metal was shown to result in a more effective material for the oxidative coupling reaction compared to MgO itself or MgO doped with reducible metal oxides (*6*). In addition catalysts prepared from the alkaline earth metal oxides and carbonates have been shown to be active for the oxidative coupling reaction of methane (*7, 8*).

In this paper the methane oxidative coupling activity resulting from supporting different loadings of Zn oxide, a nonreducible oxide, and Mn oxide, a reducible oxide, on MgO and Li_2CO_3/MgO are discussed. The relationship between activity and the physico-chemical properties of the catalysts are explored. This represents part of a comprehensive study of the activity of these catalysts doped with various transition metal oxide. The information was sought with the aim of further understanding the reaction mechanism and to enable an improvement in the Li_2CO_3/MgO catalyst activity and C_2 selectivity to be made.

2. EXPERIMENTAL

In the preparation of the catalysts, MgO powder (Strem) was added to boiling water and the mixture was continuously stirred. After 1 h, the required amount of Li_2CO_3 (Strem) was added. The appropriate amount of the transition metal nitrate, zinc or manganese, was added half an hour later. In the

[1] To whom correspondence should be addressed.

[2] Present address: Centre for Off-Campus Studies, Universiti Sains Malaysia, Penang, Malaysia.

0021-9517/91 $3.00

case of a transition metal oxide supported on MgO the procedure was repeated but no Li_2CO_3 was added.

The suspension was continuously heated and stirred until a thick paste formed. This paste was left under room conditions overnight before being dried at 120°C for 10 h. A portion of this material was then removed and set aside. Another portion was compacted at 15,000 psi to form a disk of 30 mm in diameter and 6 mm in thickness. These disks were later broken into cubes of about 6 mm in dimension and calcined in air at 900°C for 10 h in a platinum crucible. Under such conditions with a low partial pressure of carbon dioxide the lithium carbonate can decompose to the oxide (*9*). A precalcination temperature of 900°C was selected in order to achieve a stable catalytic system which would not sinter or lose material appreciably at a reaction temperature of 700–850°C. All the calcined material was ground and sieved to select a particle size less than 43 μm for the catalytic studies.

The catalytic activity of these materials was determined using a microreactor made of Alsint (Al_2O_3) operated at atmospheric pressure. The reactor was replaced at regular intervals to avoid contamination by volatile components of the catalyst. In blank experiments the methane conversion at 800°C was less than 3%, well below the value for suitable catalytically active materials. An amount of catalyst, normally 0.2 g, was used with a total gas flow rate of 25 ml/min. The partial pressures of methane and oxygen in the reactant stream were near 220 and 110 Torr, respectively, with the balance being helium. These parameters correspond to average methane flow characteristics of 36.2 ml methane/g catalyst/min. The effluent from the reactor was connected to a HP 5890 gas chromatograph. The composition of the gas was analysed using the thermal conductivity detector of the GC. Helium was used as the carrier gas at a total flow rate of 60 ml/min and the reference flow rate was 30 ml/min. Temperature-programmed treatment of the Carbosieve S column was used in order to achieve good separation between the gas components. Water is one of the major products of the oxidative coupling reaction. Since the presence of water speeds up the degeneration of the column a copper tube immersed in a 1-hexanol bath at −44°C was used to trap out most of the water. Carbon mass balances were always better than 95%.The C_3 and C_4 yields were less than 2 C mol% of product when explicitly monitored.

The composition of the prepared catalyst was determined by the atomic absorption spectroscopic method. A Varian AA1475 series atomic absorption spectrometer was used in these determinations. X-ray powder diffraction patterns of the catalytic materials were obtained with a Philips powder diffractometer. A Cu$K\alpha$ source was used under operating conditions of 40 kV and 20 mA.

Temperature-programmed reduction (TPR) was performed on the catalytic materials using a laboratory built apparatus (*10*). The reductant gas used was hydrogen, with argon as the diluent gas. The gas flow rates of 0.5 ml/min hydrogen and 5 ml/min argon were controlled by Porter electronic mass flow controllers.

The average particle size of the prepared catalyst, and the morphology of calcined sample was studied by scanning electron microscopy (SEM). A Philips 505 SEM was used for this purpose. The samples that were normally used "as prepared" for the calcined samples, or as a pressed disk for powdered samples, were gold coated prior to being studied. A Jeol JXA 50A electron microprobe analysis was used to study the surface composition of a selected catalyst. The samples were in the forms of "as prepared" or as pressed disks suitably carbon coated as for the SEM studies.

3. RESULTS AND DISCUSSION

3.1 *Catalyst Compositions and Catalytic Activity*

The compositions of the zinc oxide doped Li_2CO_3/MgO and MgO catalysts as determined by AAS are presented in Table 1.

TABLE 1

Composition of Calcined MgO and Li_2CO_3/MgO Catalysts Doped with Different Loadings of Zinc Oxide

Sample	Mol% Li	Mol% Zn
Zn1	—	0.3
Zn2	—	0.6
Zn3	—	2.2
Zn4	—	9.4
LiZn0	27.3	0.0
LiZn1	21.4	0.3
LiZn2	16.8	0.6
LiZn3	24.2	2.6
LiZn4	21.4	11.9

Data are presented on a mole percent basis relative to the magnesium loading. For reference, 21.4 mol% Li corresponds to 6.1 wt%.

The effect of zinc oxide loading on the activity of Li_2CO_3/MgO catalyst has been determined and the activity data are presented in Table 2. The results are reported after 2-h time-on-stream.

For reactions at 710 and 760°C the total methane conversions are largely independent of zinc loading. Comparing the activity of these catalysts at 805°C, it is observed that the percentage of methane conversion is near 30% except for the catalyst with 2.6 wt% zinc. The presence of zinc oxide resulted in only minor changes in total conversion relative to the undoped sample, designated LiZn0. Studies by previous researchers (*11, 12*) have demonstrated that lithium-doped ZnO catalysts can be active for methane oxidative coupling, but conversion and selectivity are usually lower than for Li/MgO catalysts under comparable conditions. In no case was full oxygen consumption achieved. At 800°C, when the zinc oxide loading was 2.6 mol%, the lowest methane conversion of around 22% was achieved although the product distribution was similar to that at other loadings. While the partial pressures of reactants were slightly lower in this case this observation provides an incomplete explanation for the discrepancy.

The activity of the zinc oxide-doped MgO catalysts at 805°C has been determined and the results are presented in Table 3. An exhaustive oxidation with full oxygen consumption occurs favouring the formation of carbon dioxide. A slight decrease in methane conversion occurs with increasing Zn loading, but this is not considered significant.

The effect of reaction temperature on the activity of samples with different loadings of zinc oxide on Li_2CO_3/MgO catalysts is also given in Table 2. Generally similar trends between the product distribution and temperature were observed over these catalysts. At low temperatures, ethane and carbon dioxide are the major products. At higher reaction temperatures the overall C_2 yield and selectivity to C_2H_4 increases.

The composition of catalysts with different loadings of Mn oxide on Li_2CO_2/MgO and MgO as determined by AAS is given in Table 4. The activity of the Li_2CO_3/MgO-doped catalyst at 805°C is affected by the Mn loading (Table 5). The presence of Mn oxide on Li_2CO_3/MgO resulted in a significant increase in the total methane conversion but not in the product quality. At a loading of 0.1 mol% Mn, the methane conversion was 36% compared with 27% for the undoped catalyst. The highest methane conversion (39%) occurred over a 0.3 mol% Mn-doped catalyst. The C_2 selectivity was near 53% compared with 64% for the undoped catalyst.

The activity data of catalysts with differ-

TABLE 2

The Activity of Calcined Li_2CO_3/MgO Catalysts Doped with Different Loadings of ZnO

T(°C)	$^pO_2$ (Torr)	$^pCH_4$ (Torr)	Conversion[a]		Carbon Selectivity[a]			
			CH_4	O_2	C_2H_6	C_2H_4	CO	CO_2
LiZn0(0.0)								
800	117	219	27	49	30.3	33.8	0.0	35.9
760			14	22	46.4	32.2	0.0	30.5
710			6	14	41.1	7.3	0.0	51.6
LiZn1 (0.3)[b]								
805	116	234	27	58	29.7	25.7	1.9	42.4
760			17	42	35.5	9.3	0.0	55.3
710			8	22	33.3	5.4	0.0	61.3
LiZn2 (0.6)								
805	112	225	30	61	28.1	33.7	1.6	36.6
760			15	27	47.6	15.9	0.0	36.6
710			5	8	47.9	12.7	0.0	29.4
LiZn3 (2.6)								
805	107	214	22	42	32.5	33.4	0.0	34.1
760			12	18	51.1	22.7	0.0	26.2
710			3	2	77.3	22.7	0.0	0.0
LiZn4 (11.9)								
805	107	224	32	75	28.0	26.1	1.6	43.3
760			17	36	45.8	10.8	0.0	43.3
710			5	6	68.6	10.3	0.0	18.1

[a] Percent.
[b] Mol% Zn. Total flow rate 25 ml min^{-1}.

ent loadings of Mn oxide on MgO at 805°C are presented in Table 6. These catalysts favour the exhaustive oxidation of methane to carbon dioxide as was the case for the ZnO/MgO systems (Table 3). Full oxygen consumption occurs even at a low manganese loading. It was also observed that at higher manganese loadings the amount of methane converted decreased slightly while selectivity to carbon dioxide increased. The

TABLE 3

The Activity of MgO Catalysts Doped with Different Loadings of Zinc Oxide at 805°C

T(°C)	$^pO_2$ (Torr)	$^pCH_4$ (Torr)	Conversion[a]		Carbon selectivity[a]			
			CH_4	O_2	C_2H_6	C_2H_4	CO	CO_2
Zn1 (0.3)[b]	107	199	29	100	9.3	0.0	0.0	90.7
Zn2 (0.6)	109	215	28	100	8.1	0.0	6.3	85.6
Zn3 (2.4)	105	207	28	100	7.3	0.0	10.0	82.7
Zn4 (9.4)	105	217	27	100	10.6	0.0	4.9	84.5

[a] Percent.
[b] Mol%. Total flow rate 25 ml min^{-1}.

TABLE 4

Composition of Calcined Li_2CO_3/MgO and MgO Catalysts Doped with Different Loadings of Manganese Oxide

Sample	Li/Mn/MgO		Sample	Mn/MgO
	Li[a]	Mn[a]		Mn[a]
LiMn1	21.7	0.1	Mn1	0.1
LiMn2	20.7	0.3	Mn2	0.4
LiMn3	22.4	2.0	Mn3	2.0
LiMn4	24.2	8.8	Mn4	9.2

[a] Mol%.

trend in CO yields with temperature was different for the two catalysts.

Higher methane conversion at all reaction temperatures was observed over Li_2CO_3/MgO doped with Mn oxide compared to the corresponding Zn oxide-doped catalytic system; however, the selectivity to C_2 compounds was generally lower at the higher conversions. A decrease in the reaction temperature resulted in a decrease in methane conversion but it was not necessarily followed by the increase in C_2 selectivity. On the catalysts with Mn loadings of 0.1 and 0.3 mol% the C_2 selectivity increases to a value of >64% with a decrease in reaction temperature to 710°C; however, the C_2 selectivity

TABLE 5

The Activity of Calcined Li_2CO_3/MgO Catalyst Doped with Different Loadings of Manganese Oxide

T(°C)	$^pO_2$ (Torr)	$^pCH_4$ (Torr)	Conversion[a]		Carbon Selectivity[a]			
			CH_4	O_2	C_2H_6	C_2H_4	CO	CO_2
LiMn1 (0.1)[b]								
805	112	233	36	84	23.6	31.4	0.0	45.1
760			24	49	35.0	25.9	0.0	39.1
710			8	15	48.6	15.8	0.0	6.7
LiMn2 (0.3)								
805	109	228	39	95	22.0	31.0	0.0	47.0
760			28	60	31.3	29.7	0.0	39.1
710			10	18	48.9	16.6	0.0	34.5
LiMn3 (2.0)								
805	111	237	38	100	21.6	26.3	0.0	52.1
760			28	73	28.4	19.4	0.0	52.2
710			11	28	37.4	11.4	0.0	51.2
LiMn4 (8.8)								
805	108	227	31	100	16.5	10.4	0.0	73.1
760			27	97	13.8	5.5	0.0	80.7
710			19	74	5.4	1.9	0.0	92.7

[a] Percent.

[b] Mol%. Total flow rate 25 ml min^{-1}.

TABLE 6

The Activity of MgO Catalysts Doped with Different Loadings of Manganese Oxide at 805°C

T(°C)	$^pO_2$ (Torr)	$^pCH_4$ (Torr)	Conversion[a]		Carbon selectivity[a]			
			CH_4	O_2	C_2H_6	C_2H_4	CO	CO_2
Mn1 (0.1)[b]	114	218	28	100	4.6	0.0	14.3	81.1
Mn2 (0.4)	105	217	28	100	6.3	0.7	10.0	81.3
Mn3 (2.0)	113	222	27	100	4.6	0.3	4.1	87.6
Mn4 (9.2)	111	223	26	100	3.1	1.4	0.0	94.5

[a] Percent.
[b] Mol%. Total flow rate 25 ml min^{-1}.

over the 8.8 mol% catalyst decreased to <8% with a decrease in reaction temperature to 710°C. The carbon oxides selectivity over these catalysts at all temperatures is exclusively to carbon dioxide in contrast to the case when Li is not present (Table 5). These results demonstrate that while Mn oxide on Li_2CO_3/MgO promotes the overall conversion of methane more effectively than the zinc oxide dopant the product distribution is not as beneficial since the Mn-based catalyst shows increased combustion activity.

The results in Table 5 serve to demonstrate that selectivity and conversion are influenced by the Mn doping levels on the catalyst. This effect is associated with the physical and chemical changes occurring on the Mn oxide-doped Li_2CO_3/MgO catalysts. At a Mn loading of less than 2.0 mol%, the high C_2 selectivity and the similar product distribution trends with reaction temperature are consistent with the surfaces of these catalysts being chemically similar to those for the undoped Li_2CO_3/MgO catalyst, or for the Zn oxide-doped Li_2CO_3/MgO catalyst. The increase in methane conversion over these catalysts relative to the undoped Li_2CO_3/MgO or the Zn oxide-doped Li_2CO_3/MgO catalyst can be related to surface physical changes outlined in the next section. Over the 8.8 mol% catalyst, however, the surface must be chemically different to those with lower loadings. This is confirmed by SEM studies. The increase in exhaustive oxidation of methane over this catalyst (Table 5) is consistent with the findings for the Mn oxide/MgO samples (Table 6) and results from manganese oxide in a high oxidation state being present on the surface during the reaction. The manganese oxide may be involved in a redox process and hence facilitate oxygen transfer on the catalyst surface. The mechanism apparently increases the conversion of methane to carbon dioxide. The zinc ion predominantly exists in an oxidation of +2 and is not reducible under the reaction conditions (*13*); hence a redox process involving ZnO is highly unlikely. An alternative explanation is required for the exhaustive oxidation of methane over ZnO/MgO catalysts (Table 3). An increase in surface defects as a consequence of the doping may be the explanation. Surface areas are in general too small (1–5 m^2 g^{-1}) to play a significant role. Furthermore, the findings do not reveal a significant variation with zinc oxide loading.

3.2 Physico-Chemical Properties

3.2.1 *Zn oxide-doped MgO and Li_2CO_3/MgO systems.* The surface layer coating on the precalcined (900°C for 10 h) but unground Zn oxide-doped Li_2CO_3/MgO samples was studied by scanning electron microscopy (Fig. 1). This was done to gain an insight into surface layer formation, an effect which is less clearly visible but still

present after grinding the samples for activity studies. The undoped Li_2CO_3/MgO shows evidence of a surface coating layer (Fig. 1a) due to carbonate melting (*9*) relative to an uncalcined sample, not shown, where a distribution of particles was evident mainly in the range from 0.1 to 1 μm. A few of the individual particles are still evident in Fig. 1a. At low loadings of zinc, LiZn1 (0.3 mol%), the surface layer increases, Fig. 1b, and is similar in appearance to the overlayer for the undoped sample LiZn0. When the zinc loading is substantially increased as for LiZn4 (11.9 mol%) a major change in the surface morphology is observed. The micrograph for LiZn4 at lower magnification ($\times$203) reveals a honeycomb-type surface network while the structure revealed at the same magnification ($\times$5000) as Fig. 1a–1b shows the underlying MgO particles preserving much of their original integrity but with some fusing together.

In order to further characterise the Zn oxide-doped Li_2CO_3/MgO catalyst, electron microprobe analyses of the various forms of these materials have been studied in (Table 7). The calcined samples are prepared (C) and after being ground to a powder (P) were examined. The activity studies were performed on the powdered samples. The analysis of the powdered form of the calcined sample (P) should represent more closely the composition of the bulk. The difference between the calcined (C) and powdered (P) samples should indicate the changes that occurred near the surface of the calcined catalysts as a result of precalcination, since the Li-rich layers encapsulating the particles are thicker than the X-ray escape depth. Micrographs of the powdered samples (not shown) reveal a material with particles of similar size to the original MgO crystallites, but more irregular in shape.

On the Li_2CO_3/MgO catalyst doped with Zn oxide the microprobe analyses performed were for the determination of Mg and Zn content while on the Mn oxide-doped catalyst the analyses were for Mg and Mn. The values for Li present given in Table 7 were calculated by difference. The calcined Zn oxide-doped analyses yielded a much higher content of Zn than for their calcined and powdered counterpart. For example, the calcined LiZn4 sample is predicted to have 11.4 mol% Zn in the layers analysed which is close to the stoichiometric value while the value for the corresponding powdered sample is reduced to 2.3 mol% Zn. There is an enrichment of the surface layers with Zn oxide and Li_2CO_3 relative to the MgO phase during the precalcination stage. The higher average percentage deviation in the mol% of Mg on calcined samples relative to the powdered form (typically a factor 5–10) is due to the Li_2CO_3 phase being unevenly distributed on the sample surface. Evidence for Li segregation has also been obtained from some preliminary XPS studies.

The XRD patterns for samples with different loadings of ZnO on MgO and on Li_2CO_3/MgO have been determined. No XRD pattern for the ZnO phase was observed for the doped MgO indicating that the ZnO exists as small crystallites or is in an amorphous form. On the doped Li_2CO_3/MgO catalysts, at low loadings of Zn oxide the major features are consistent with the presence of MgO and Li_2CO_3. At higher ZnO loadings the XRD patterns changed considerably and the presence of an independent ZnO phase is indicated. These observations are consistent with the electron micrographs, Fig. 1b and 1d.

In the activity studies it was observed that Zn oxide on MgO promoted the exhaustive oxidation of methane to carbon dioxide. The presence of Zn oxide on MgO is not likely to result in a major increase in the redox ability of the catalyst. The temperature-programmed reduction technique was used to confirm the absence of reducible sites on the zinc oxide-doped MgO and Li_2CO_3/MgO catalysts. The TPR profiles of ZnO-doped MgO catalysts revealed no reducible phases while those for zinc oxide-doped Li_2CO_3/MgO catalysts (Fig. 2a, 2b) were typical of the Li_2CO_3 decomposition profiles observed

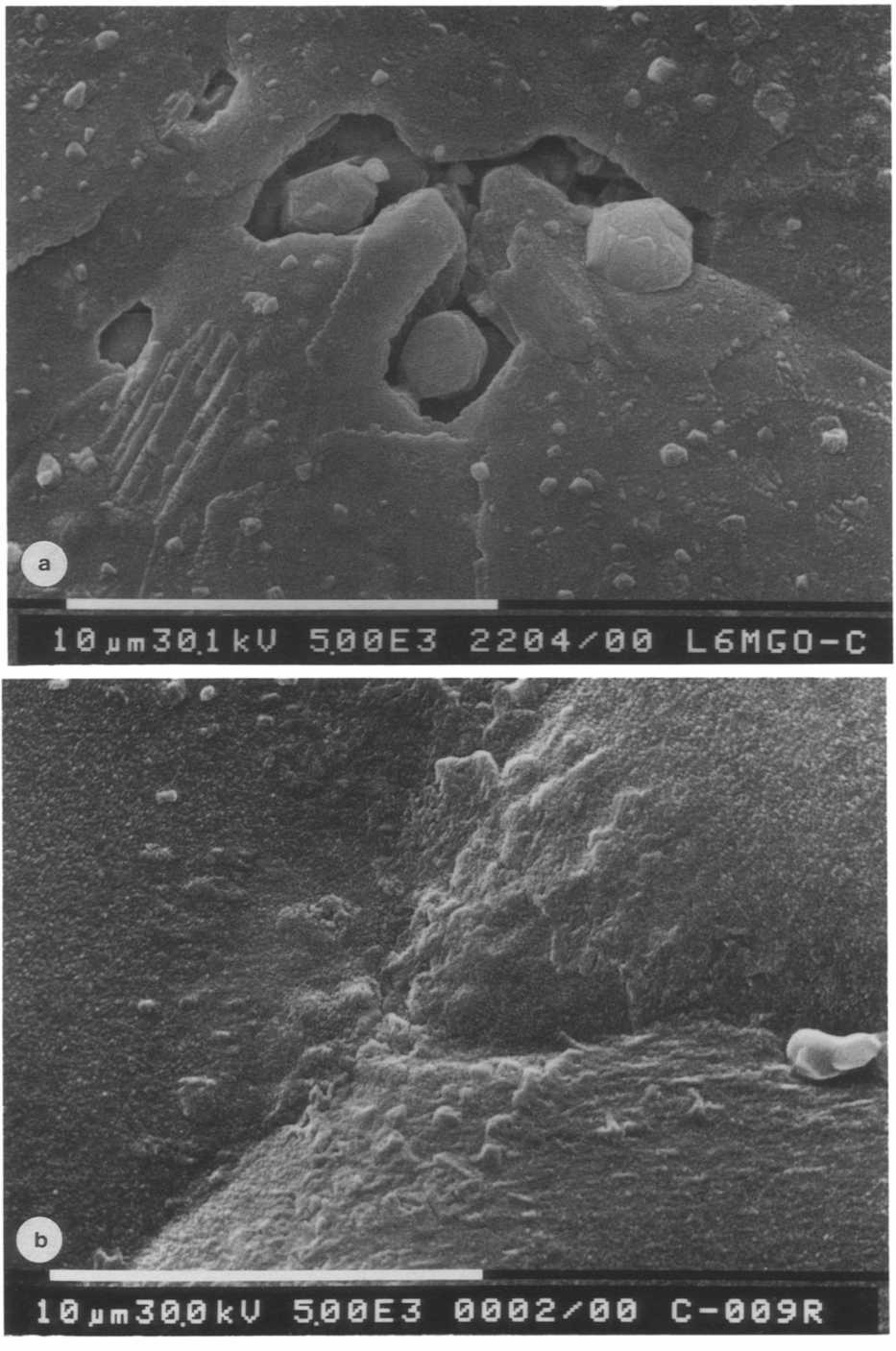

FIG. 1. SEM micrographs of Li_2CO_3/MgO catalysts doped with different loadings of Zn oxide after precalcination at 900°C for 10 h. (a) LiZn0 (×5000); (b) LiZn1 (×5000); (c) LiZn4 (×203); (d) LiZn4 (×5000).

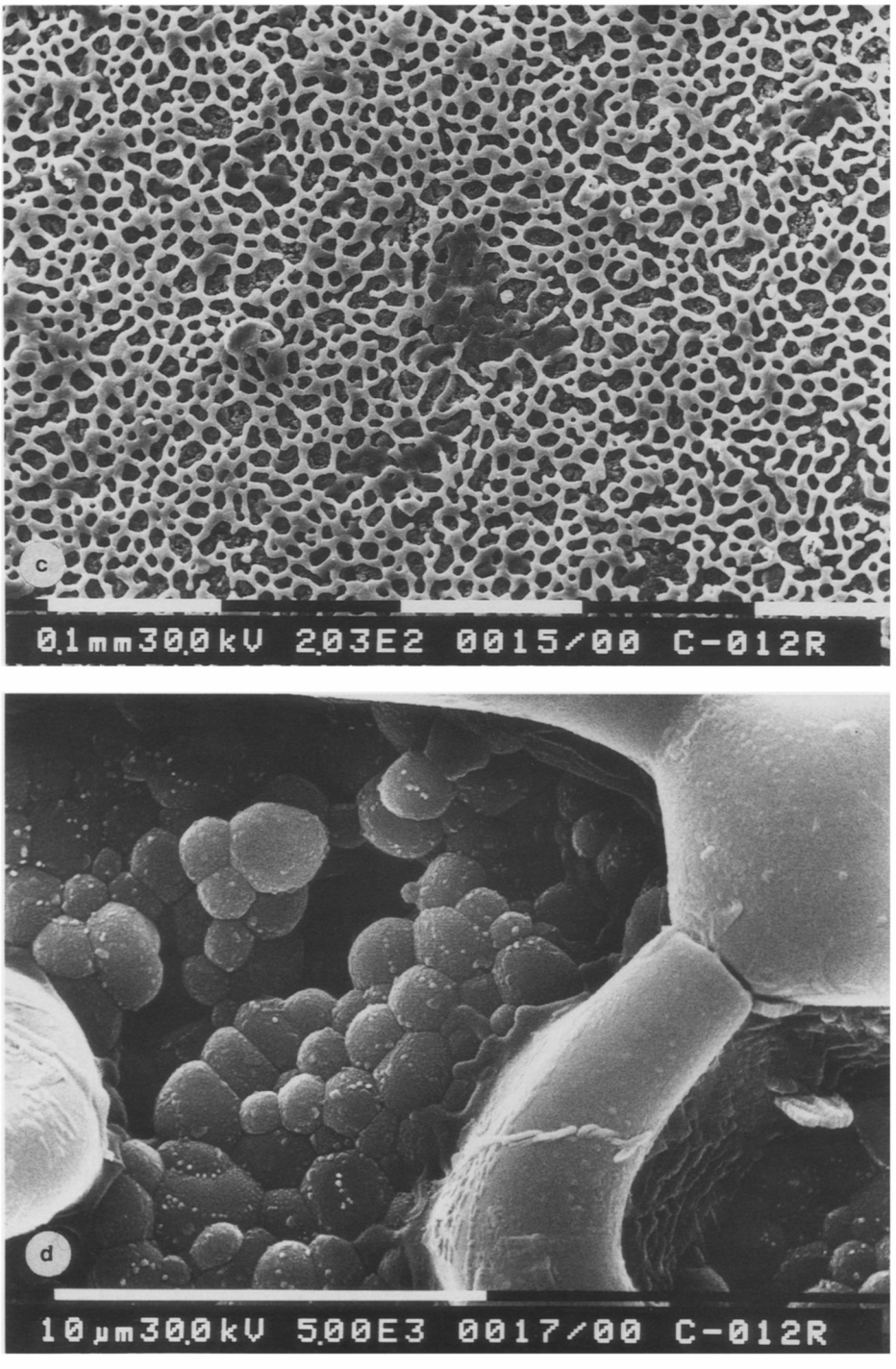

FIG. 1—*Continued*

TABLE 7

Composition of Calcined and Powdered Li_2CO_3/MgO Catalysts Doped with Zn and Mn Oxides

Catalyst	Mg	Mol% (microprobe)[a] Zn or Mn	Li[b]
LiZn2-C	24.8(7.1)[c]	1.5(6.1)[c]	73.7
LiZn2-P	80.2(1.2)	0.2(5.7)	19.6
LiZn3-C	44.8(7.8)	2.8(0.5)	52.4
LiZn3-P	76.7(1.5)	0.4(2.2)	22.9
LiZn4-C	24.6(23.8)	11.4(4.6)	64.0
LiZn4-P	71.0(2.2)	2.3(4.4)	26.7
LiMn2-C	34.6(12.3)	0.2(7.1)	65.2
LiMn2-P	80.2(1.6)	0.4(2.9)	19.4
LiMn3-C	57.1(9.1)	2.3(4.1)	40.6
LiMn3-P	66.6(1.2)	2.0(2.8)	32.4

Note. C, calcined. P, calcined and ground to a powder <43 μm.

[a] Values determined by microprobe analysis.

[b] The difference between 100% and (Mg + metal values).

[c] Average % deviation from three analyses.

on an undoped Li_2CO_3/MgO catalyst, that is, a small peak (I) at around 800°C followed by a major peak (II) at around 850°C. The TPR profiles of the used LiZn3 catalyst also indicated the absence of any new reducible sites. An increase in the size of the Li_2CO_3 decomposition profiles (Fig. 2d) of the used LiZn3 catalyst further confirms the enrichment of the surface with Li_2CO_3 under reaction conditions.

3.2.2 *Manganese oxide-doped MgO and Li_2CO_3/MgO systems.* The presence of Mn oxide on Li_2CO_3/MgO has a detrimental effect on the Li_2CO_3 layer formation of the catalyst samples after the precalcination as indicated by comparison of the micrographs Figs. 1a–1b with Fig. 3a at the same magnification and transition metal loading. On the 0.3 mol% catalyst-LiMn2, some extended surface layer was present (Fig. 3a) but on samples with higher Mn loadings no such extended structure was observed (Fig. 3b). At the higher Mn oxide loadings the particle size increases significantly relative to the parent MgO due to the fusing of particles (Fig. 3b). The presence of manganese oxide does not appear to stabilise the extended carbonate layer that normally coats the Li_2CO_3/MgO catalyst sample after 10 h precalcination at 900°C. The electron microprobe analyses (Table 7) show that there is surface enrichment in the Li and Mn species for the calcined samples relative to the MgO phase, but the Li enrichment is not as great as when the sample was doped with a comparable amount of ZnO.

The XRD patterns for Mn oxide-doped MgO and Li_2CO_3/MgO catalysts have been determined. The patterns for Mn1 and Mn2 show only the presence of crystalline MgO. The XRD pattern of the 2 mol% Mn/MgO (Mn3) catalyst is consistent with the presence of the Mn_3O_4-type phase. The XRD patterns of LiMn1 and LiMn2 indicate that the catalyst consists mainly of MgO and Li_2CO_3. The XRD pattern for the 2.0 mol% Mn on the catalyst LiMn3 is consistent with the presence of $MgMnO_3$, while the peaks in the XRD pattern of 8.8 mol% catalyst are consistent with the presence of a Li_2MnO_3 peak.

The TPR profiles of the Mn oxide-doped MgO and Li_2CO_3/MgO catalysts are presented in Fig. 4. The analyses are undertaken to identify the primary initial species which are present. The reaction conditions for the methane coupling reaction are clearly different from those used for the TPR

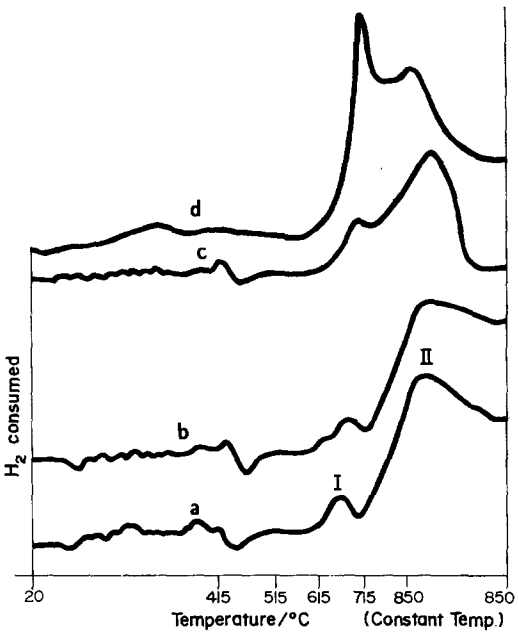

FIG. 2. TPR and decomposition profiles of Zn oxide-doped Li_2CO_3/MgO catalysts. (a) LiZn2; (b) LiZn3; (c) LiZn4; (d) used LiZn3.

sequence. The subsequent reductions identified by TPR are unlikely to occur precisely as presented here under methane coupling conditions especially when there is not complete consumption of oxygen. However, TPR and XRD studies of the used catalysts do indicate a reduction in the metal oxide species. At a low loading of Mn oxide on MgO, the TPR profiles show a broad reduction peak between 300 and 600°C. In the TPR profiles of the Mn3 catalyst (Fig. 4a) a sharp reduction peak between 600 and 700°C together with possibly broad reduction peaks at lower and higher temperatures were observed.

The TPR patterns of the Mn oxide-doped Li_2CO_3/MgO with increasing Mn loadings (Fig. 4b, 4c, and 4d) show the presence of reduction peaks together with peaks due to Li_2CO_3 decomposition. The TPR profile of the used 2.0 mol% Mn on Li_2CO_3/MgO and 2.0 mol% Mn on MgO are given in Figs. 4e and 4f respectively.

For the purposes of discussion the main TPR peaks have been labelled I, II, III. The other features are due to the Li_2CO_3 decomposition (see Fig. 2) and are not discussed further. The reduction sequence identified by comparison with TPR studies of the parent Mn oxides, thermodynamic considerations, and the XRD data reported above is as follows.

$$\text{I} \quad 2MnO_2 + H_2 \rightarrow Mn_2O_3 + H_2O$$
$$\text{II} \quad 3Mn_2O_3 + H_2 \rightarrow 2Mn_3O_4 + H_2O$$
$$\text{III} \quad Mn_3O_4 + H_2 \rightarrow 3MnO + H_20$$

This information provides the basis for the interpretation of Fig. 4 recognising that factors such as hydrogen pressure, flow rate, and heating rate as well as the distortion caused by the underlying decomposition of the Li_2CO_3 phase can affect the position of the TPR peaks.

Figure 4a for the Mn3 sample predominantly reflects the reduction of a Mn_2O_3 (II)- and/or Mn_3O_4 (III)-type phase in the temperature range 515–615°C. The LiMn2 and LiMn3 samples with lower loadings of Mn have a TPR peak (Fig. 4b, 4c) corresponding to the reduction of MnO_2 near 430°C (I). The area of the peak reflects the increased amount of the Mn oxide on the surface of the $LiMn_3$ catalyst (Table 7). The second reduction peak near 680°C corresponds to stages II and III of the Mn oxide reduction in the presence of the lithium salt, but is also influenced by the carbonate decomposition. The TPR profile for the LiMn4 sample with the highest Mn loading (8.8 mol%) is somewhat different than the other profiles (Fig. 4d). The XRD evidence is consistent with a Li_2MnO_3 phase being present; furthermore the earlier profiles (Fig. 4b, 4c) show that peak I moves towards higher reduction temperatures with an increase in Mn oxide loadings. Hence, the profile is interpreted as the reduction of some free MnO_2 (I) followed by the reduction of a Mn oxide species which is strongly influenced by the presence of lithium. The profile is also altered by the decomposition of the lithium carbonate in the same temperature range.

For the 0.3 mol% Mn catalyst the reduc-

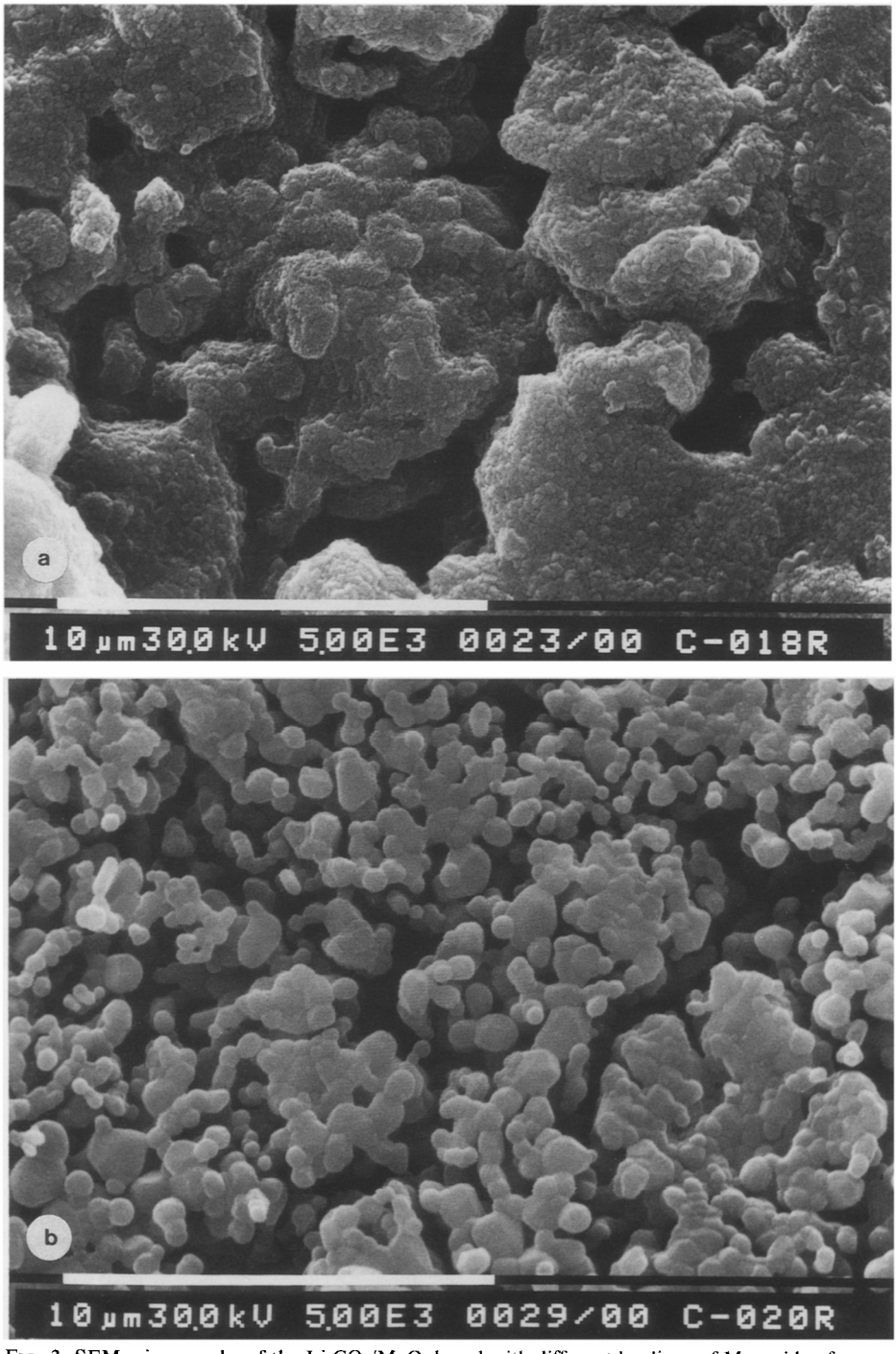

FIG. 3. SEM micrographs of the Li_2CO_3/MgO doped with different loadings of Mn oxide after precalcination at 900°C for 10 h. (a) LiMn2 (×5000); (b) LiMn4 (×5000).

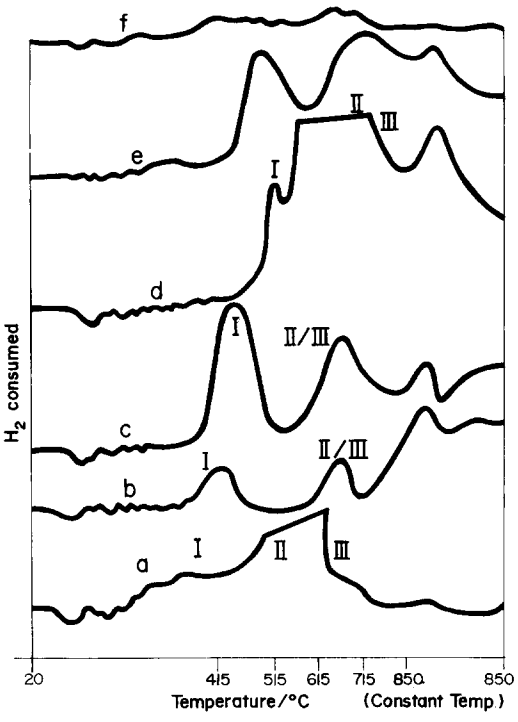

FIG. 4. TPR and decomposition profiles of Mn oxide-doped MgO and Li_2CO_3/MgO catalysts. (a) Mn3; (b) LiMn2; (c) LiMn3; (d) LiMn4; (e) used LiMn3; (f) used Mn3.

tion peak (Fig. 4b) at 430°C corresponds to phase I while that at 690°C corresponds to phases II and III. The intensity of these peaks increased at higher Mn loadings (Fig. 4c). At a loading of 8.8 mol% (Fig. 4d), the peak near 700°C becomes more dominant while the peak at lower temperatures decreases in intensity. It was also observed that the lower temperature reduction peak moves towards higher temperature with an increase in manganese oxide loadings. The reduction peaks are assigned as outlined above for the Mn oxide/MgO system. The exhaustive oxidation behaviour for the LiMn4 and Mn4 catalysts is consistent with this interpretation. The peak at around 420°C in Figs. 4b and 4c may be due to the presence of a Li_2MnO_3 phase.

The position and area of peak I on the used catalyst (Fig. 4e) is altered compared with the fresh material. This observation is consistent with a decrease in the reducible manganese oxide species on the surface after 2 h of use under the reaction conditions. The shift in peak position to higher temperature is consistent with the Mn species interacting more strongly with the underlying Li–Mg matrix.

3.3 Relationship between Physicochemical Properties with Catalytic Activity

The physical and chemical characteristics of the Li_2CO_3/MgO catalysts were influenced by the presence of the transition metal oxides. The SEM micrographs of the catalytic sample indicate that the oxide doping influenced the formation of a surface layer on the calcined samples. In the Mn oxide case doping also disrupts the interaction between Li_2CO_3 and MgO making the resulting material easier to grind. Particles of the ground Mn oxide-doped Li_2CO_3/MgO catalyst were smaller and more spherical in shape compared to ground particles of the undoped Li_2CO_3/MgO catalysts. For the Zn oxide-doped Li_2CO_3/MgO catalysts the interaction between MgO and Li_2CO_3 was not significantly disrupted. As a result, when ground, the particles of this catalyst are of a size similar to that of the undoped oxide, i.e., in the range 0.1 to 1.0 μm.

It was observed from TPR experiments that the Mn oxide phases on doped Li_2CO_3/MgO are available for reduction and hence the redox Mn sites can influence the surface oxidation of methane. The presence of redox sites facilitates the oxygen transfer resulting in higher exhaustive oxidative reaction activity on the Mn oxide-doped Li_2CO_3/MgO catalyst. This is especially evident at high Mn loadings (Table 5). The decrease of selectivity to C_2 hydrocarbons can be linked to the presence of these sites. Surface area changes were considered too small to play a significant role in the variation observed.

The catalytic activity of MgO has been observed to be significantly influenced by the preparative method, by dopants, and by the pretreatment procedure. This parent

material and the ZnO/MgO systems (Table 3) also promote exhaustive oxidation possibly via surface defects. For the ZnO-doped Li_2CO_3/MgO systems the total conversion and high selectivity to C_2 hydrocarbons was retained but not significantly enhanced with increasing Zn loading. At best, an interaction between ZnO and Li_2O or Li_2CO_3 may stabilise the catalyst against lithium loss at reaction temperature. Other researchers (*12, 13, 15*) have found Li_2CO_3/ZnO systems to have good methane oxidative coupling activity.

4. CONCLUSION

The catalytic selectivity of Mn oxide-doped Li_2CO_3/MgO catalysts for the oxidative coupling of methane to C_2 products was significantly affected by metal loading, while a lesser effect was observed for ZnO-doped systems. Disruption to the carbonate surface layer and the existence of a TPR reducible phase was observed on the Mn oxide system. These factors influence C_2 selectivity by promoting exhaustive oxidation. Of the two classes of catalysts investigated the Zn-doped systems are to be preferred because at 805°C they consistently yield a methane conversion of >25% and a selectivity of C_2 hydrocarbons of near 60%. However, they are not superior to the undoped Li_2CO_3/MgO system. The Mn-doped catalysts have a higher activity at 805°C, but a lower C_2 selectivity.

ACKNOWLEDGMENTS

We thank Mr. M. E. Hughes for his technical assistance and Dr. M. J. Ridd for scientific discussions.

REFERENCES

1. Driscoll, D. J., and Lunsford, J. H., *J. Phys. Chem* **89,** 4415 (1985).
2. Ito, T., and Lunsford, J. H., *Nature* **314,** 72 (1985).
3. Kimble, J. B., and Kolts, J. H., *Chem. Tech,* 50 (1987).
4. Hutchings, G. J., Scurrell, M. S., and Woodhouse J., *J. Chem. Soc. Chem. Commun.,* 186 (1987).
5. Roos, J. A., Bakker, A. G., Bosch, H., van Om men, J. G., and Roos, J. R. H., *Catal. Today* **1** 133 (1987).
6. Moriyama, T., Takasaki, N., Iwamatsu, E., and Aika, K., *Chem. Lett.,* 1165 (1986).
7. Aika, K., Moriyama, T., Takasaki, N., and Iwamatsu, E., *J. Chem. Soc. Chem. Commun.,* 121 (1986).
8. Aika, K., Moriyama, T., Fujimoto, N., Takasaki N., and Iwamatsu, E., *Sixth Int. Symp. Heterog Catal. Proc. Sofia* **1,** 418 (1987).
9. Larkins, F. P., and Nordin, M. R., *Appl. Spec trosc.* **42,** 906 (1988).
10. Roe, G., Hons. Thesis, University of Tasmania 1986.
11. Otsuka, K., Liu, Q., Hatano, M., and Morikawa A., Chem. Lett., 903 (1986).
12. Zhang, H. S., Wang, J. X., Driscoll, D. J., and Lunsford, J. H., *J. Catal.* **112,** 366 (1988).
13. Bhasin, M. M., *Stud. Surf. Sci. Catal.* **36,** 34 (1988).
14. Matsuura, I., Utsumi, Y., Nakai, M., and Doi, T. *Chem. Lett.* 1981 (1986).
15. Roos, J. A., Korf, S. J., Bakker, A. G., de Bruijn N. A., and van Ommen, J. G., *Stud. Surf. Sci Catal.* **36,** 427 (1988).